International Journal of Pressure Vessels and Piping 192 (2021) 104388

Contents lists available at ScienceDirect

International Journal of Pressure Vessels and Piping

journal homepage: http://www.elsevier.com/locate/ijpvp

Comparison of sensitivity measures in probabilistic fracture mechanics

Klaus Heckmann [a,*], Robertas Alzbutas [b], Min Wang [c], Tatjana Jevremovic [d], Bengt O.Y. Lydell [e], Jürgen Sievers [a], Xinjian Duan [c]

[a] Gesellschaft für Anlagen- und Reaktorsicherheit (GRS) gGmbH, Cologne, Germany
[b] Lietuvos Energetikos Institutas (LEI), Kauno Technologijos Universitetas (KTU), Kaunas, Lithuania
[c] Candu Energy Inc., Mississauga, Ontario, Canada
[d] International Atomic Energy Agency (IAEA), Vienna, Austria
[e] Sigma-Phase, Inc., Vail, AZ, USA

ARTICLE INFO

Keywords:
Probabilistic fracture mechanics
Sensitivity
Parameter ranking
Nuclear technology

ABSTRACT

Probabilistic fracture mechanics (PFM) simulates the behavior of cracked structures and propagates uncertainties from input parameters to a failure probability or its uncertain estimate. In nuclear technology, this approach supports the assessment of the rupture probability of highly reliable pipes, which is an important parameter for the safety analysis of a nuclear power plant. For the appropriate probabilistic modelling of a structure with consideration of uncertainties, but also for the analysis of PFM application cases, the question arises, which input parameter of a probabilistic model has a higher impact on the estimate of computed failure probability, and which has a minor impact. This question is associated with the sensitivity measures or importance factors of the input parameters and their ranking concerning their influence.

In this paper, six different approaches for the quantification of the sensitivity of parameters PFM evaluations are investigated: the amplification ratio, the direction cosine, the degree of separation, the analysis of the most probable failure point, the separation of uncertainty method, and the simple sample-based sensitivity study. Each method is described, visualized, applied to a common test case, and compared. The application case and the comparison are part of the Coordinated Research Project (CRP), "Methodology for Assessing Pipe Failure Rates in Advanced Water-Cooled Reactors (AWCRs)" by the International Atomic Energy Agency (IAEA), which is dedicated to the development of failure rates of piping in AWCRs. The participants used different PFM computer codes to analyze the test case and individual sensitivity methods to rank the input parameters, which motivated the comprehensive survey.

The predicted parameter ranking of the approaches is consistent between the methods and between different PFM codes, but the approaches differ in the scope and the required effort. A conclusion is drawn and recommendations for the six different approaches are given.

1. Introduction

PFM is an engineering discipline that can be used as an approach for the structural reliability assessment of mechanical components and systems (see e.g. Ref. [1] for a recent review). In this approach, a fracture mechanics analysis of crack initiation, crack growth, and failure is used to simulate degradation processes in a structure. Uncertainties of data are partially included by considering probabilistic distribution functions as input parameters, and then propagates through various analytical models with uncertainty, and finally, failure probabilities are estimated. The study of pipe failure frequencies and its computation by consideration of structural mechanics can be seen as a part of the field of structural reliability, more precisely a time-variant structural reliability analysis [2].

The underlying approach is the computational simulation of a structure and the assessment of its failure. The behavior of a structure is characterized by multiple basic variables $x_1,\ldots,x_n$, collected in a vector $x = (x_1, \ldots, x_n)$. A function $g(x)$ describes the structural state, with a criterion for failure as $g(x) \leq 0$. The set $\{x : g(x) = 0\}$ is called the limit state. Each basic variable x_i is distributed according to a (cumulative) distribution function F_i and the associated probability density function ρ_i. The joint probability density function of all basic variables is $\rho(x)$. The

* Corresponding author. Gesellschaft für Anlagen- und Reaktorsicherheit (GRS) gGmbH, Schwertnergasse 1, 50667 Cologne, Germany.
E-mail address: Klaus.Heckmann@grs.de (K. Heckmann).

https://doi.org/10.1016/j.ijpvp.2021.104388
Received 17 August 2020; Received in revised form 15 March 2021; Accepted 18 March 2021
Available online 28 March 2021

failure probability is then given by the integral over the failure area.

$$p = \int_{g(x)\leq 0} \rho(x)dx \tag{1}$$

In the case of the temporal evolutions of structures, which are relevant for long operations and ageing effects, the scope has to be extended to a time-variant reliability problem. In the time-variant approach, the parameter sets become time-dependent, becoming a trajectory $x(t)$ in parameter space. The estimate of failure probability in such an approach is the transition probability of trajectories crossing the limit state. For this, the estimate of failure probability after a time t is introduced, $p(t)$. The failure probability density at a given time is defined as the temporal derivative, $\dot{p}(t)$. Often, it is convenient to define also the failure frequency f_{t_a,t_b} with respect to a finite interval $[t_a, t_b]$ instead of an infinitesimal time – the annual failure frequency is an example of this.

$$f_{t_a,\,t_b} = \frac{1}{t_b - t_a}\int_{[t_a,\,t_b]} \dot{p}(t)dt = \frac{p(t_b) - p(t_a)}{t_b - t_a} \tag{2}$$

Since Equation (2) is a numerical evaluation of the probability density over the time interval $[t_a,t_b]$, the failure rate can be evaluated by introducing the survival function in the denominator as follows,

$$\lambda_{t_a,\,t_b} = \frac{p(t_b) - p(t_a)}{(t_b - t_a)[1 - p(t_a)]} \tag{3}$$

When the time interval $t_b - t_a$ is one year, the numerical evaluation of the annual failure frequency and the failure rate are simplified as

$$\begin{aligned} f_{t_a,t_a+1} &= \frac{1}{\text{year}}[p(t_a+1) - p(t_a)] \\ \lambda_{t_a,t_a+1} &= \frac{1}{\text{year}}\frac{p(t_a+1) - p(t_a)}{[1 - p(t_a)]} \end{aligned} \tag{4}$$

In the limit of small probabilities ($p(t) \ll 1$), these two expressions in Equation (4) are closely related, $f_{t_a,t_a+1} \approx \lambda_{t_a,t_a+1}$.

Traditionally, many methods used to calculate the structural reliability, such as the First-Order Reliability Method (FORM) or Second-Order Reliability Method (SORM), are based on the Most Probable Failure Point (MPFP) (see Ref. [2] for a review article or [8] for a textbook). The MPFP represents the most likely combination of random input variables that result in failure. The MPFP (also called the design point, most probable point, or beta point) is a point in the basic variable space defined as the point in the failure area with the highest probability density.

$$D = \text{argmin}\|x\|\big|_{g(x)\leq 0} \tag{3}$$

The norm $\|\cdot\|$ is defined in the standard normal space (also called reduced space or u-space). Each basic variable x_i with cumulative distribution function F_i can be transformed into a standard normally distributed parameter u_i by the Gaussian distribution function Φ.

$$u_i = \Phi^{-1}(F_i(x_i)) \tag{4}$$

The norm introduced above is just the Euclidean norm of the variable transformed to the standard normal space, and the norm of the MPFP is denoted by the reliability index β.

$$\|x\|^2 = \sum_i u_i^2 \tag{5}$$

A structural reliability case may have more than one MPFP; in this case, Equation (3) defines a set of points. The MPFP represents the parameter set for which the failure is most likely to occur – thus the parameter set can be interpreted as the typical constellation of influences that are relevant for failure.

The function $g(x)$ and the limit state is, for the scope of this paper, redefined, that a failure occurs within the considered time frame. A sketch of the two variable space, the probability density function, and the time-variant limit state are shown in, which represents the conceptual basis for the methodology described in Section 2.

For the analysis of sensitivity and importance of computed quantities, sensitivity measures and importance factors are the key tools to investigate dependencies, influences, and correlations. There are different importance factors and sensitivity indices, like Pearson's ordinary correlation, Spearman's rank correlation, Blomqvist's medial correlation, and Kendall's rank correlation, and dedicated software tools for their computation, [3]. However, there is a remarkable difference in the application of sensitivity measures for general deterministic and probabilistic computations. The beforementioned well-established importance factors and sensitivity indices are constructed for deterministic input parameters and deterministic target quantities, and measuring its relation and dependence. For PFM, a relevant issue is the specification of distribution functions of the input parameters and the key results are estimates of probabilities of structural failures. The deterministic sensitivity approaches are neither considering the probability density functions of the basic variables as an intrinsic uncertainty nor the geometrical properties of a structural reliability approach (as depicted in Fig. 1). This motivated individual uncertainty analyses within probabilistic structure mechanical computations and approaches tailored to the structural reliability problem were proposed [1,4]. A similar situation exists in probabilistic safety assessment, where individual importance measures are proposed [5].

When comparing sensitivity measures in PFM, it is important to consider the different use cases of sensitivity investigations. In general, and not only in PFM, sensitivity analysis can support design and optimization decisions. A sensitivity study of the failure rate can tell how the reliability is changed if an investigated subject is slightly modified (what-if scenarios), like the geometrical thickness of a structure to be varied, an alternative material to be used, or the maintenance plan to be changed. In probabilistic structural reliability analysis, it is often important to identify which input uncertainty is relevant for the estimate of final failure probability, and which input quantity uncertainty is of minor importance concerning structural failure. This analysis can reveal at which point it is beneficial to reduce uncertainty, for instance by increased quality measures or additional research. It can also support the understanding of the estimate of resulting failure probability: If a key influencing quantity is affected by the tail sensitivity problem [15], the absolute value of the failure frequency should be discussed only very carefully. Hence, the sensitivity investigations in PFM can be classified into two categories: One related to intentional parameter variations (which could be referred to as sensitivity study), and the other related to uncertainties in parameters (which would be referred to as sensitivity analysis in a strict sense). Although they provide both a parameter ranking for the influence on the estimates of failure probabilities and have technical similarities, the scope and the application case for both are not identical. If the sensitivity analysis is narrowed to the distributed input parameters of a PFM case, the selection of parameters to be included in a sensitivity comparison is not a subjective choice, but

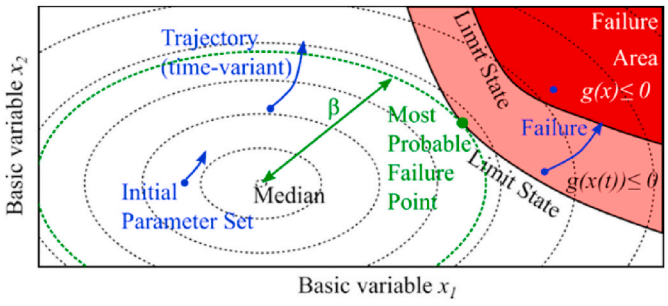

Fig. 1. Illustration of the general approach of probabilistic structural reliability. The dark failure area corresponds to the initial time, while the light failure area indicates the range where trajectories will enter the failure area.

uniquely given by the case definition.

The aim of this paper is to provide the comparison of different methods, measures, and factors for the identification of relevant parameters in a probabilistic fracture mechanics evaluation. The selected methods specifically characterize the sensitivity in PFM input data rather than general parameter ranking approaches. This objective is in alignment with the International Atomic Energy Agency (IAEA) Coordinated Research Project (CRP) "Methodology for Assessing Pipe Failure Rates in Advanced Water-Cooled Reactors (AWCRs)". In this CRP, organizations from Canada, Germany, Lithuania, Malaysia, Russia, South Korea, Tunisia, and the United States of America develop a technical basis for the assessment of plant reliability parameters. Within the application of PFM as a methodology for the prediction of failure rates in water-cooled reactors within the CRP, three organizations provided results for the sensitivity ranking of PFM applications, providing the basis for the paper.

This paper is organized in a sequence of theory, calculation, results, and discussion. In Section 2 (theory), six individual sensitivity methods which were proposed specifically for PFM are presented in a comprehensive way togehter with a graphical interpretation related to each approach. This theory section is shown at an abstract, conceptual level. In Section 3 (calculation), a probabilistic fracture mechanics case study as a demonstration object for the theoretical concepts, the computational tools, and the failure analysis results are presented. Note that the actual background of the PFM case in Section 3 is of minor importance; its role is to provide a representative case for the method comparison. Section 4 (results) shows the parameter ranking results of the individual methods, while Section 5 (discussion) concludes with a summary, outlook, and recommendations.

2. Methods

In this study, six different methods for the ranking of relevant influence/importance parameters are compared. The individual methods are discussed in the following subsections on a conceptual level – the actual application of the methods within a case study is shown in Section 4.

2.1. Amplification ratio

The first technique (in alphabetic order) for quantitative importance analysis is based on the amplification ratio V [6], with the generalization proposed in Ref. [7]. The amplification ratio is a vector, with one entry for each basic variable i.

$$V_i = \frac{\max\left\{p|_{x_i=x_-}, p|_{x_i=x_+}\right\}}{p}, x_\pm = F_i^{-1}\left(\frac{1}{2} \pm Q\right) \tag{6}$$

The quantity $p|_{x_i=z}$ denotes the probability of failure, computed by setting the ith basic variable to the fixed value $x_\pm$ using specific restrictions. This value is determined by the cumulative distribution function F_i of the variable. In two dimensions, these restrictions of basic variables correspond to lines parallel to the axes, as shown in Fig. 2.

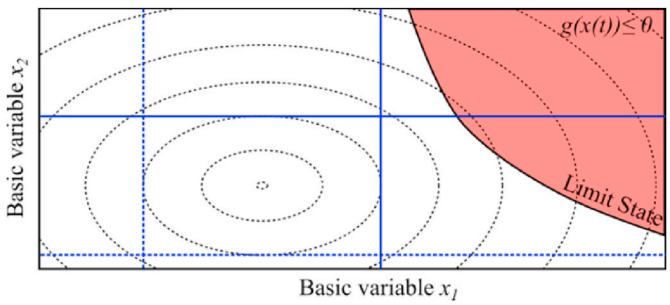

Fig. 2. Illustration of the evaluations for the amplification ratio.

The original amplification ratio proposed by Ref. [6] is obtained by taking the 5% and 95% quantile, i.e. $Q = 0.45$. The amplification is useful for identifying basic variables that have a strong effect on the resulting estimate of failure probability. An amplification ratio of 1 for one parameter indicates that the parameter, even with the statistical scattering, is not relevant for the estimation of failure probability. Amplification ratios larger than 1 indicate that the parameter affects the estimate of failure probability. Especially for small total failure probabilities, an amplification ratio of zero is typical for a parameter with a strong effect on the result. An application of the amplification ratio concept to highly reliable nuclear pipes can be found in Ref. [7].

2.2. Direction Cosines Method

The direction cosines are based on the position of the MPFP (see Section 1). In the reduced (or standardized) space, they measure the sensitivity or importance of the failure probability to the corresponding random variable [9]. The more sensitivity of the failure to the random variable, the more important the variable is. In highly non-linear problems, the determination of MPFP can become quite complex and Monte Carlo Simulation (MCS) may be a more plausible method than a direct computation of the MPFP. In the Direction Cosines Method (DCM), the MPFP is represented by averaging the realizations of each variable that lead to failure in the Monte Carlo simulation.

The DCM importance factor of each random variable in term of the square of direction cosine $(\cos^2\alpha_i)$ is calculated for a random variable that is normally distributed:

$$\cos^2\alpha_i = \frac{\tilde{u}_i^2}{\sum_i \tilde{u}_i^2} \tag{7}$$

and

$$\tilde{u}_i = \frac{\mu_{f,i} - \mu_i}{\sigma_i}, \tag{8}$$

where

$\cos\ \alpha_i$: direction cosine of the ith variable;
$\mu_{f,i}$: mean of the ith random variable corresponding to the failures;
μ_i: mean of the ith random variable;
σ_i: standard deviation of the ith random variable.

For any probability distribution other than the normal distribution, μ_i and σ_i are obtained by use of the "equivalent normal distribution" as described by Ang and Tang [10]. The mean and the standard deviation of this equivalent normal distribution are implicitly given by the condition that the density function ρ_i and the cumulative distribution F_i match at the MPFP D.

$$\Phi\left(\frac{D_i - \mu_i}{\sigma_i}\right) = F_i(D_i), \frac{1}{\sigma_i}\phi\left(\frac{D_i - \mu_i}{\sigma_i}\right) = \rho_i(D_i) \tag{9}$$

Hence, the equivalent normal distribution has to be found numerically, and it depends on the MPFP location. The MPFP and the difference to the estimate μ_f, as well as the angles α_i in the two-dimensional standard example are visualized in Fig. 3.

The MPFP corresponds to the smallest value of $\beta = \sum_i u_i^2$ and can be used to estimate failure probability. In DCM, the realizations that caused failure are known from Monte Carlo simulations and the average values of these realizations are used to evaluate the equivalent normal distribution for sensitivity or importance analysis.

2.3. Degree of separation method

Degree of Separation Method (DSM) is similar to DCM except that the mean value (μ_i) and the standard deviation (σ_i) in Equation (4) are estimated from all realizations sampled in the simulation rather than those of user-defined input distributions, that is

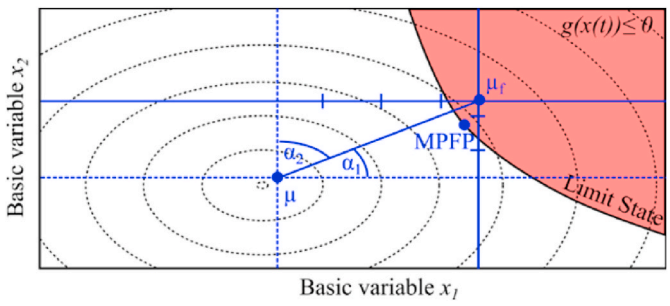

Fig. 3. Illustration of the α_i in the DCM, with the different positions of the real MPFP and the approximation μ_f. Note the different scale tics on the two bars.

$$v_i = \frac{\mu_{f,i} - \mu_{all,i}}{\sigma_{all,i}} \tag{10}$$

The DSM importance factor is:

$$\gamma_i = \frac{v_i^2}{\sum_i v_i^2}, \tag{11}$$

where

γ_i: importance factor of the ith variable;

$\mu_{all,i}$: mean of all realizations of the ith random variable;

$\sigma_{all,i}$: standard deviation of all realizations of the ith random variable;

$\mu_{f,i}$: mean of realizations of the ith random variable resulting in failure.

The illustration provided in Fig. 3 is also suitable for the DSM, as only the computation of μ, σ, and μ_f differ. In the degree of separation method, the consideration of equivalent normal distributions is not required. However, the following strategy [4] is often used for calculating $\mu_{f,i}$, $\mu_{all,i}$ and $\sigma_{all,i}$:

1. If the distribution of the input variable is normal, the mean and the standard deviation are of the actual values.
2. If the distribution of the input variable is log-normal, $\mu_{all,i}$ and $\sigma_{all,i}$ are computed by the mean and the standard deviation of the logarithm of the realization values x_j, respectively ($\mu_{f,i}$ is obtained by restricting the sum to realizations leading to failure).

$$\mu_{all,i} = \frac{1}{N}\sum_{j=1}^{N} \log x_{i,j}, \sigma_{all,i} = \sqrt{\frac{1}{N}\sum_{j=1}^{N} \left(\log x_{i,j} - \mu_{all,i}\right)^2} \tag{12}$$

3. For other distributions, if the range of sampled values is large, step 2 is used; step 1 is used otherwise. The range is quantified as the ratio of the maximum and the minimum of the sampled values. If the ratio is greater than 10, the range is considered large.
4. Skewness or Kurtosis can also be used to determine the treatment of the input variable. If skewness or kurtosis is low, the input variables can be treated as Normal distribution, else the input variable can be treated as Log-normal.

The idea of the DSM is that if the distribution of the realizations leading to failure of a random variable is farther away from its overall distribution of all realizations than another random variable, the random variable is more important than others. One advantage of this method compared to the DCM is its simplicity of sensitivity or importance estimation. Also, no prior knowledge of the parameters of the probability distribution is required as the distribution is characterized by the actual sampled values during the Monte Carlo simulation.

2.4. Analysis of the MPFP

Another structural reliability technique is the position analysis of the MPFP (design point analysis). The position of the MPFP D, with respect to the median of each basic variable i, $F_i^{-1}(0.5)$, is the opportunity to measure the influence of each parameter: A basic variable with high influence will differ much from the median at the MPFP, while a parameter with low influence will differ little (or not) from the median value at the MPFP. For a comparison of different quantities, it is recommended to transform the variables to standard normal variables u_i (see Equation (4)). The ranking relation (establishing a mathematical preorder on the parameter indices) can be written as follows.

$$i \geq j \Leftrightarrow \left|\Phi^{-1}(F_i(D_i))\right| \geq \left|\Phi^{-1}(F_j(D_j))\right| \tag{13}$$

In this notation, parameters of a "higher" index have a higher influence on the result. An illustration of the MPFP and its position analysis is shown in Fig. 4.

As several advanced sampling techniques rely on MPFP, the MPFP information is often a natural output of a reliability computation. The analysis of the MPFP for a probabilistic analysis is recommended to check if this parameter set is meaningful [15]. An application and analysis of subsequent consequences of a MPFP for a fracture mechanics evaluation are found in Ref. [16].

The analysis of the MPFP for a sensitivity ranking relation has also limitations. The case $D = 0$ (which is interpreted that failures are very often) is a limitation, but not relevant for the most interesting case of highly reliable piping with small failure probabilities. A more relevant case is the existence of multiple distinct local minima of the limit state norm. In this case, each of this local MPFP would define an own parameter ranking, and the global ranking between MPFP is not directly possible. Another complication appears if in-service inspections and repair effects are considered by the probability weight adaption of each sample in case of an inspection, changes the shape of the u-space. This problem is avoided, however, by implementing the detection probability during an inspection by an additional random variable instead of using sample weight corrections.

2.5. Separation of uncertainty method

A two-loop code architecture for the treatment of the uncertainties [11,12] as shown in Fig. 5 is implemented in several PFM codes. This architecture allows the uncertainty to be propagated separately: the aleatory uncertainty propagates through the inner loop and the epistemic uncertainty propagates in the outer loop. The topics of how to distinguish and how to separate the two uncertainties are beyond the scope of this paper; however, interested readers are referred to Ref. [13], which provides a generalized discussion of the treatment of aleatory and epistemic uncertainties.

With the two-loop code architecture, a failure probability curve (referred to as a hair) is produced for each epistemic realization (set). As a result, a number of hairs are generated from this type of code architecture. The mean and the percentile of the failure probability estimate

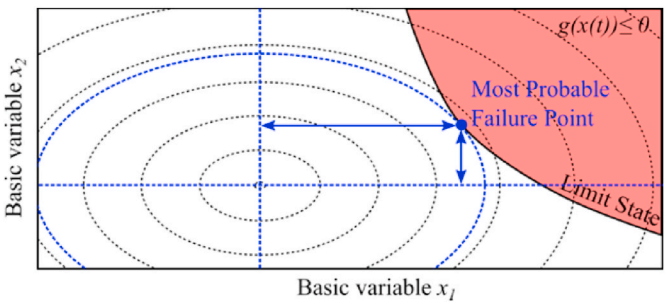

Fig. 4. Illustration of the MPFP analysis.

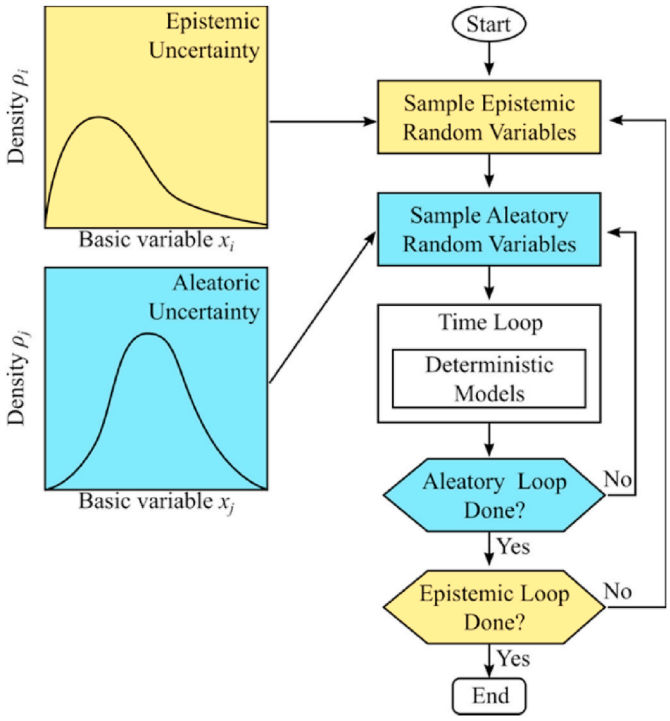

Fig. 5. Flow chart of two-loop treatment of uncertainty.

are calculated from the statistical treatment of all of the hairs. The epistemic realizations used for the produced hairs are shown in the standard example in Fig. 6.

The scatter of the hairs represents the contribution of the epistemic uncertainty to failure probability. The wider the hairs scatter, the more contribution the epistemic uncertainty has. Therefore, the two-loop simulation can be used to study the importance of the random variables or the importance of uncertainty of parameters. This allows to study of the effects of an individual random variable but also compounds the effects of multiple random variables through the nested two-loop code architecture.

2.6. Simple sample-based sensitivity study

The uncertainty analysis uses a simple sample-based sensitivity study with variations of main influencing parameters. It is just a simplification of probabilistic sample-based sensitivity analysis of uncertainty. The main influencing parameters of pipe rupture in the nuclear context include structural reliability models, considering a range of various dimensions, materials, degradation mechanisms, and loading conditions.

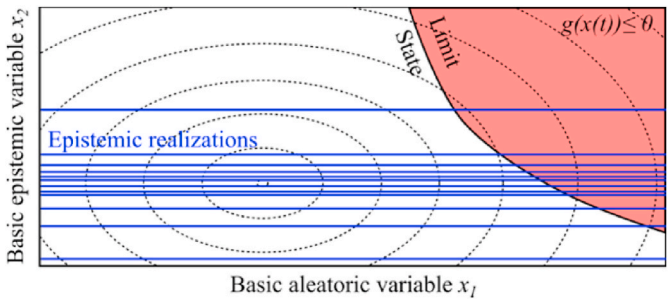

Fig. 6. Illustration of the Separation of Uncertainty method, assuming that the basic variable x_1 is aleatoric and x_2 is epistemic. Horizontal (blue) lines symbolize epistemic realization, and for each of them, hairs are computed. (For interpretation of the references to colour in this figure legend, the reader is referred to the Web version of this article.)

The sensitivity analyses are performed to evaluate the influence of foreseeable variations and uncertainties, which requires an individual assessment and modelling for each quantity. This assessment of variations and uncertainties may include initially distributed (basic variables) and initially non-distributed quantities of the application case, and also the grouping or combination of variations if correlations are expected (see Table 1).

Based on the anticipated variations and uncertainties, three levels (at least) are considered for each parameter: Low/Baseline/High, where baseline represents the original parameter set, Low numerically smaller, and High numerically higher values – alternatively, the Low/High nomenclature can refer to the expected structural performance or risk in the test case. For the quantitative analysis, a specific sensitivity matrix of parameters is established, where only 1 parameter is varied, others are at the baseline level. A scheme of this parameter variation for the simple sample-based sensitivity study is shown in Table 2, it is similar to the system used in Ref. [14].

An illustration of the variation of probability density functions is shown in Fig. 7. The variated distribution functions lead to variations of the probability weight within the failure region, which leads to a variation of the failure probability.

The probabilistic computation is repeated with each parameter definition from the sensitivity matrix, and the change in the total failure probability is compared. A parameter with high influence will cause a large variation in failure probability, while a parameter with small influence will cause a minor change in the probability.

The choice of the actual levels for the High and Low levels is to a certain extend up to the user. With a certain choice, a metric on the space of input parameters is established and can be compared, and it is clear that the resulting sensitivity ranking will be affected by this definition. If the High and Low levels are defined by the use of a common factor for all parameters, the result will represent sensitivity with respect to relative changes. If the levels are chosen guided with knowledge about the actual physical system and possible uncertainties, the resulting variation will directly correspond to the possible variation of the reliability in the actual system.

3. Application case

In this section, a PFM application case is defined and analyzed in short as a demonstration object for the sensitivity measure approaches presented in Sec. 2. The application case was chosen as a representative PFM problem with sufficient, but limited complexity, to allow a fair and concise comparison of sensitivity measures, which is the central aim of this paper. Consequently, it is not the aim to motivate or to question the case definitions and their assumptions, but important aspects which are intentionally left out in this investigation will be discussed critically in Sec. 5.2.

3.1. Test case

The test case was part of a benchmark study for the comparison of probabilistic fracture mechanics methods [17]. It represents an austenitic stainless steel pipe weldment of a small diameter spray line in a pressurized water reactor (PWR) nuclear power plant. The pipe has an outer diameter of 114 mm and a wall thickness of 10.8 mm. The material

Table 1
Different sensitivity measures for deterministic and probabilistic.

Analysis Type	Deterministic	Probabilistic
Input	Input Values	Distributions
Output	Function of Input	Probabilities
Uncertainties	Additional Estimate	As given by the Distributions
Sensitivity	Classical rankings	See Sec. 2

Table 2
Parameter variation scheme of the sensitivity matrix for the simple sample-based sensitivity study.

	Parameter 1	Parameter 2	…
Base	B	B	B
Parameter 1	L	B	B
	H	B	B
Parameter 2	B	L	B
	B	H	B
…	B	B	…
	B	B	

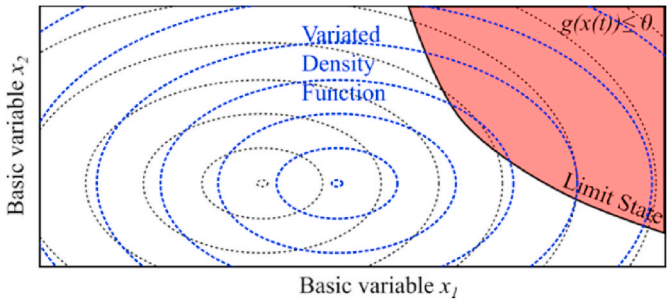

Fig. 7. Illustration of the simple sample-based sensitivity study: one initially distributed parameter is changed to the High level, while all others remain at the baseline values.

is characterized by a modulus of elasticity of 177 GPa and a Poisson ratio of 0.3. The material strength is modeled by normally distributed parameters for yield stress, ultimate stress, and fracture toughness. The means (μ) and standard deviations (σ) for the three quantities are given in Table 3.

The pipe is operated at an internal pressure of 15.41 MPa, the axial membrane stress σ_p due to this pressure is 31.8 MPa. Additional axial stresses σ_b from bending and thermal expansion accumulate to an additional 33.7 MPa in total. The through-thickness distribution of weld residual stresses in the axial direction is given in Fig. 8.

The initiation and growth of internal circumferential cracks due to stress corrosion cracking are postulated in this line. The crack initiation frequency is assumed to be 1/(2451 years), with a size of an initiated crack of 1 mm in depth and an exponentially distributed crack length of the mean value of 30.95 mm (truncated to the maximal length of the full perimeter). The relation between the crack growth rate and the stress intensity factor K_I is modeled by a power law.

$$\frac{da}{dt} = \begin{cases} C_{SCC} K_I^{n_{SCC}} & K_I \le K_{thr} \\ C_{sat} & K_I > K_{thr} \end{cases} \tag{14}$$

The parameters of this relation are shown in Table 4. Operation time of 8000 h per year is assumed, with a total lifetime of 60 years.

This discussion is restricted to the base case of the evaluation; the effect of in-service inspection and leak detection is not addressed here, for further information, it can be referred to Ref. [17].

3.2. Computation and results

The benchmark case was evaluated with different codes. The

Table 3
Distributed material characteristics.

Characteristic		μ	σ
Yield Stress	[MPa]	130	13
Ultimate Stress	[MPa]	495	30
Fracture Toughness	[MPa $m^{1/2}$]	182	14

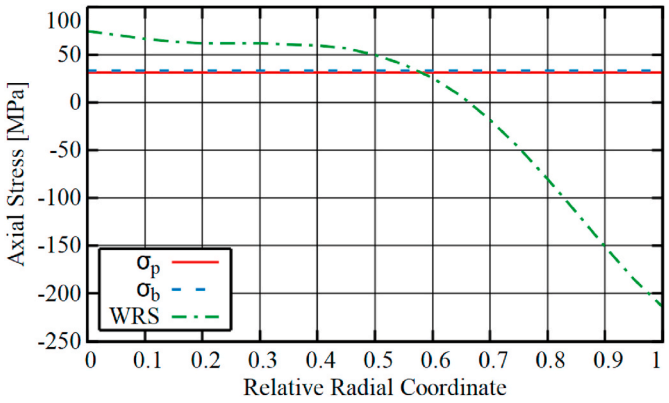

Fig. 8. Stresses and weld residual stress profile.

Table 4
Parameters of the crack growth relation.

Prefactor	C_{SCC}	$1.05 \cdot 10^{-14}$	(MPa $m^{1/2}$)$^{-5.76}$ mm/s
Exponent	n_{SCC}	5.67	–
Saturation Value	C_{sat}	$1.74 \cdot 10^{-6}$	mm/s
Threshold	K_{thr}	26.7	MPa $m^{1/2}$

Gesellschaft für Anlagen-und Reaktorsicherheit (GRS) used the self-developed PROST code [18,19], the Lithuanian Energy Institute (LEI) used the PIFRAP/AutoPIFRAP code [20–22], while Candu Energy used the PRAISE-CANDU software [11,12,23]. The codes computed the estimates of annual leak frequency as a function of the operation time, $f(y) = f_{y,y+1}$ in the sense of Equation (4). The PROST code used, for this specific result, a Monte Carlo simulation. The computed failure times are sorted in a histogram with 1-year bins to generate the time-dependent annual leak frequency. In general, PIFRAP is also able to use various time steps; in the present analysis to emphasize a basic trend a relatively large time interval is used to obtain the annual leak frequency. PRAISE-CANDU uses a 1-month time step in the calculation and a classical Monte Carlo simulation. The result of this evaluation is shown in Fig. 9.

From this graph, it can be seen that the (nearly) constant initiation frequency leads to the initiation and subsequent growth of stress corrosion cracks. The first (significant) failures are observed by all codes before the 10th year of the operation, and after that, the estimate of leak

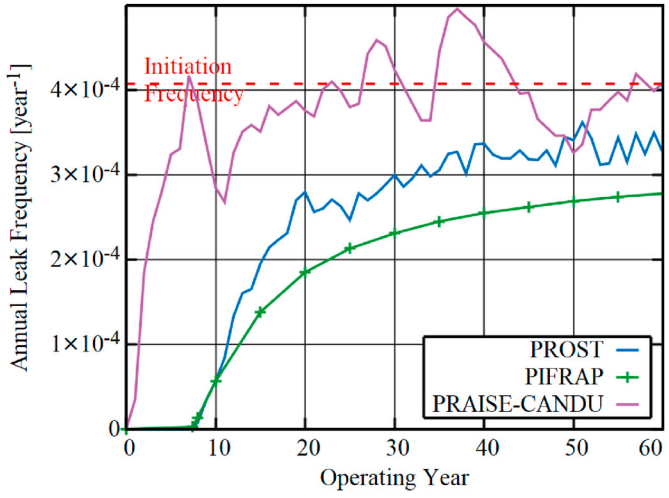

Fig. 9. Annual leak frequency as defined in Eq.(4) of the application example, computed with different codes.

probability per year increases. For infinite operations times, one could assume that the initiation value could be the saturation of this increase, and in the simulation, all three codes see that the initiation frequency is attaining this value. The agreement between the results of the different codes is good, but not perfect – this issue was discussed in Ref. [17] in more detail. The noise-like scattering of the results is a consequence of code properties, sample size, and averaging size for the generation of the histogram.

As a preparation for the parameter ranking analysis, the parameter plane of initiation frequency and initial crack length is shown in Fig. 10. For this graphical representation of the basic parameter space, parameter sets were evaluated systematically with the PROST code and recorded if any failure occurs. From this plot, it can be seen that failure occurs for early initiations and long initial cracks. Shallow cracks that initiate late in the operation will not lead to leaks. This figure, which corresponds to the abstract concept shown in the selected test case, allows us to discuss the different sensitivity measures in the following Section 4.

4. Results of individual sensitivity measures

In this section, the different methods presented in Section 2 are applied to the case study of Section 3. The analysis of the information of each one as well as the differences are discussed in Section 4.

4.1. Amplification ratio

The amplification ratio was computed with the PROST code, which is capable to compute the ratio automatically, i.e. to compute the required parameter variations, to perform the probabilistic simulation, and to compare the results for the evaluation of Equation (6). For this study, it was computed for the 5%/95% quantiles and the 1%/99% quantiles. The amplification ratio is a vector of the same dimension as the basic parameters. The two amplification ratio results are shown in Table 5.

The three material characteristics have, in both cases, an amplification ratio of unity, which can be interpreted in such a way that the failure probability is not influenced if the parameter is changed. Thus, these parameters are of minor (or even zero) importance, and the discussion can concentrate on the remaining two. The initial crack length amplification ratio moderately increases to 1.58 for both cases. This number represents the relative increase of the leak probability if the initial crack length is increased to larger values. From Fig. 10, it can be seen that the failure at the 95% quantile (93 mm) and the 99% quantile (142 mm) of the crack length, leaks occur even at later initiation times than at the median (21 mm), and this additional parameter window increases the probability of failure. The case for the initiation time is more involved. At the 5% quantile (126 years), no cracks will initiate within the operation time, and hence no leaks will occur – this leads to a leak probability and consequently to an amplification ratio of zero. (Theoretically, it is not exactly zero, because failures may occur even without a crack if the material properties are so bad that the pipe fails without crack under operational load. The PROST software is able to consider this effect even though the associated probability is really low, but as this scenario is not realistic, it is not considered further here.) The 1% quantile of the initiation time is at 25 years, thus completely in the operation time. In the parameter variation for this amplification ratio, all cracks initiate within the operation time, and consequently, the leak probability increases strongly by a factor of 43.2.

Independent of the chosen quantile, the parameter ranking as given by the amplification ratio is clear. The most important parameter is the initiation time, followed by the initial crack length. The yield stress, the ultimate stress, and the fracture toughness have equal (and minor) importance.

Table 5
Amplification ratio.

Quantiles	5%/95%	1%/99%
Yield Stress	1	1
Ultimate Stress	1	1
Fracture Toughness	1	1
Initiation Time	0	43.2
Initial Crack Length	1.58	1.58

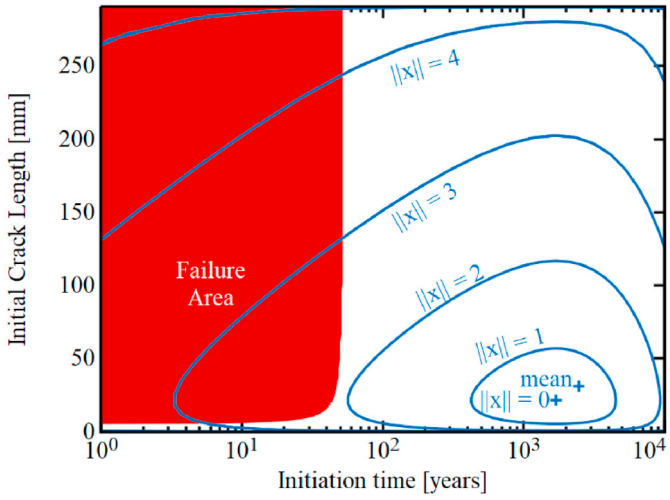

Fig. 10. Parameter subspace of the PFM analysis with failure region (red) and contour lines of the probability distribution functions corresponding to a constant integer x. The mean and median are indicated by crosses. (For interpretation of the references to colour in this figure legend, the reader is referred to the Web version of this article.)

4.2. Direction Cosines Method

In PRAISE-CANDU Version 2.0, the inputs required to calculate the estimate of failure probability are different from what is defined for the test case in Section 3.1. The failure criteria are either net-section collapse or J-tearing. Therefore, instead of using ultimate strength and fracture toughness K_{Ic}, the flow strength, and fracture toughness J_{Ic} were used. Also, the half initial crack length is input to the simulation. The five random parameters used in PRAISE-CANDU for the test case are listed in Table 6.

A simulation with 10^5 realizations was performed and all random realizations were output for the importance ranking. The importance factors of five random variables were calculated following the method described in Section 2.2, especially Eq. (7) and (8), and are listed in Table 7. Since the initiation time and a half initial crack length are defined as exponential distribution, the mean (μ_i) and standard deviation (σ_i) in Table 7 were calculated for the equivalent normal

Table 6
Distribution parameters of material properties in PRAISE-CANDU.

Characteristic	Unit	Distribution Type	μ	σ	Correlation with Flow Strength
Yield Strength, σ_y	MPa	Normal	130	13	0.5
Flow Strength, σ_f	MPa	Normal	312.5	16.3	–
Fracture Toughness, J_{Ic}	MJ/m^2	Normal	0.2069	0.0317	0.5
Initiation Time, t_I	year	Exponential	2451	2451	
Half Initial Crack Length, b_0	m	Exponential	0.0155	0.0155	–

Table 7
Importance factors of random variables using DCM; results in parentheses are obtained from the equivalent normal distributions.

	σ_y (MPa)	σ_f (MPa)	J_{Ic} (MJ/m^2)	t_I (Year)	b_0 (m)
$\mu_{f,i}$	129.7	312.0	0.2174	27	0.0162
μ_i	130	312.5	0.2069	(191)	(0.0100)
σ_i	13	16.3	0.0317	(71)	(0.0163)
u_i	−0.02	−0.03	0.33	−2.29	0.38
$\cos^2\alpha_i$(%)	0.01	0.02	1.98	95.39	2.61

distribution, see Eq. (9).

Negative values of u_i correspond to basic variables where a low value leads to failure (such as initiation time), whereas positive u_i correspond to basic variables where high values are As it can be seen from the last row in Table 7, the most important parameter is the initiation time, followed by the initial crack length. The material properties have minor importance.

4.3. Degree of separation method

Similar to DCM, the importance factors of the five random variables are calculated from the output of PRAISE-CANDU using DSM and are presented in Table 8. In DSM, the mean and the standard deviation of the distribution were estimated from all realizations with log-transformation for initiation time (t_I) and half initial crack length (b_0), while in DCM, the mean and standard deviation of the (equivalent) normal distribution were used.

Negative values have the same interpretation as in the previous section. As it can be seen from the last row of Table 8, the most important parameter is the initiation time, followed by the initial crack length. The material properties have minor importance. This is consistent with the ranking of importance using DCM.

4.4. MPFP analysis

The design point was computed with the PROST code. The 5-dimensional vector of the result is shown in Table 9 and also in Fig. 11. It can be seen that all but the initiation time coordinate are equal to the corresponding median value.

The design point of this specific problem indicates that the parameter set with the highest probability weight which leads to a leak is constructed by starting from the median value and shifting parallel to the initiation time axis. For the parameter ranking according to Equation (3), this result implies that the most influential parameter is the initiation time, whereas all other parameters are of equal (and less) importance. With regard to Fig. 10, this result ignores that the initial crack length indeed affects the failure surface, as the limit state is not entirely parallel to the axis. For this specific problem, the design point approach for the sensitivity analysis is just not capable to pay tribute to this fact.

4.5. Separation of uncertainty method

The separation of uncertainty method (SUM) selects one random variable each time as an epistemic variable in general. The realizations of the selected epistemic random variable are sampled in the outer loop,

Table 8
Importance factors of random variables using DSM obtained from the realizations (with log-transformation for t_I and b_0).

	σ_y (MPa)	σ_f (MPa)	J_{Ic} (MJ/m^2)	t_I (Year)	b_0 (m)
$\mu_{f,i}$	129.7	312.0	0.2174	3.0	−4.6
$\mu_{all,i}$	129.6	311.8	0.2172	7.2	−4.7
$\sigma_{all,i}$	13.0	16.3	0.0228	1.3	1.1
ν_i	0.010	0.011	0.008	−3.265	0.092
γ_i (%)	0.001	0.001	0.001	99.919	0.079

Table 9
MPFP coordinates, with the transformation to the standard normal variable.

	D_i		$\Phi^{-1}(F_i(D_i))$
Yield Stress	130	MPa	0
Ultimate Stress	495	MPa	0
Fracture Toughness	182	MPa m1/2	0
Initiation Time	44.7	Years	−2.1
Initial Crack Length	21.5	Mm	0

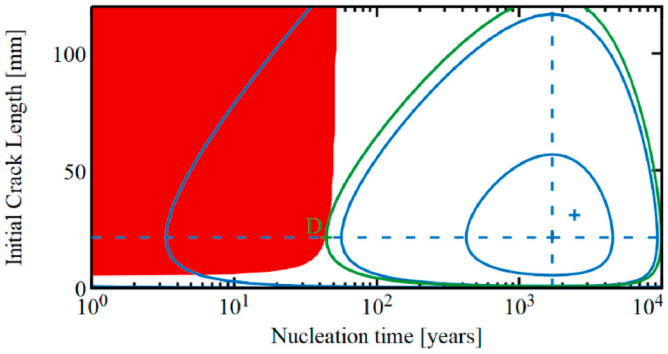

Fig. 11. MPFP position D in the subspace of two basic parameters.

while the realizations of the others are sampled in the inner loop. For the sensitivity study of this test case, three simulations were performed for crack initiation time (t_I), half initial crack length (b_0), and material properties (σ_y,σ_f, and J_{Ic}) to be the epistemic variable respectively. Each simulation consists of 10^3 epistemic realizations (outer loops) and 10^5 aleatory realizations (inner loops). The reason that three material properties were treated as epistemic variables simultaneously is that they are correlated random variables. The simulation results are presented for the initial crack length and material properties in Fig. 12. The gray curves (hairs) are results from 10^3 epistemic realizations, and the scatter of the hairs can be characterized using the width between the 5th percentile and 95th percentile in red curves.

The importance of the random variables can easily be visualized from the typical plots as shown in Fig. 12 and can be quantified by the ratio of the 95th percentile to the 5th percentile of the probability of rupture at the end of life. The ratios for the initial crack length and the material properties are 1.55 and 1.07, respectively. The result of the

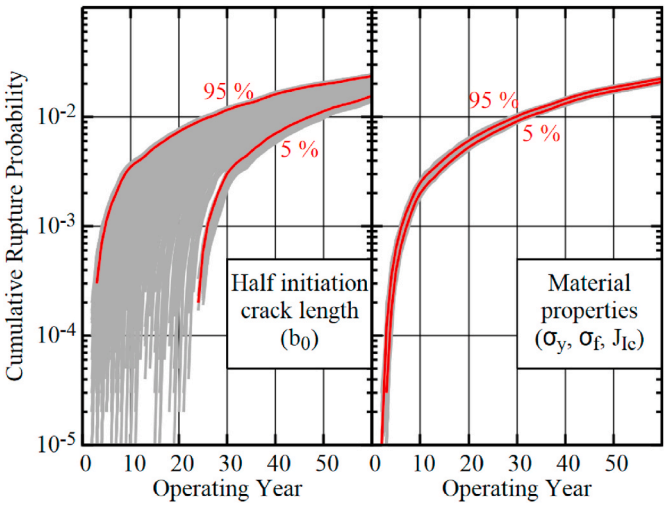

Fig. 12. Probability of failure with epistemic uncertainty; the corresponding graph for initiation time as epistemic uncertainty would show a constant zero function.

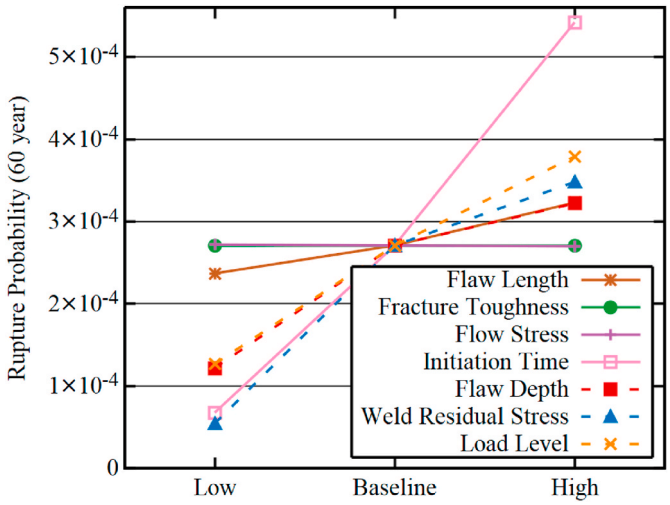

Fig. 13. Result of the simple sample-based sensitivity study with parameter variation of flaw depth, weld residual stress, fracture toughness, flow stress, load level, flaw length, and initiation time. The target parameter is the estimate of rupture probability in the year 60.

crack initiation shows that both 5th and 95th percentiles are zero because only about 25 of 10^3 cracks (less than 10%) are expected to be nucleated within 60 years for the given crack initiation frequency (1/2451 per year). This indicates that the initiation time has a very high influence on the results since only specific values from the tail of its distribution function enable failures. Therefore, from the above analysis, the rank of the importance is crack initiation time (t_I) followed by the initial crack length (b_0) while the material properties (σ_y,σ_f, and J_{Ic}) only have minor importance.

4.6. Simple sample-based sensitivity study

The simple sensitivity study for the sample-based uncertainty analysis was performed considering the test case described in Sec. 3. The selected parameters can be divided into two groups:

- Related to possible data uncertainty due to the degradation process (e.g. crack size and growth rate);
- Related to uncertainty in loading and strength; material properties, primary and secondary loads (WRS);

For analysis, the specific sensitivity matrix of parameters was used, where three levels were considered: Low/Baseline/High – the trend of the level corresponds to the change in the estimate of failure probability, not in the actual parameter. The levels High and Low are defined as scaling factors with respect to the baseline level, the actual factor is chosen with respect to the associated data uncertainty or plausible variations. The factors are summarized in Table 10 – the fact that they are not the same for all will affect the resulting estimate of probability levels, as described in Sec. 2.6.

Based on these results, the initially distributed parameters with the most influence on the result is the initiation time, while the corresponding initially non-distributed parameters are the load level and the weld residual stresses. Note that weld residual stress variation for the Low-level has a pronounced scaling factor, compared to the others. The flaw depth (initially non-distributed) and the flaw length (initially distributed) are of intermediate importance. Since the flow stress variation (initially distributed) has no visible impact in the figure; it is hence a parameter of low influence. This evaluation shows that the sensitivity of initially distributed and initially non-distributed quantities are to be discussed separately but can be numerically compared to each other.

Table 10
Parameter levels of low risk and high risk for the sensitivity study.

Parameter		Value	
		Low	High
Flaw depth		0.5	3.0
Flaw length		0.67	3.0
Load level	Pressure	0.67	2.0
	Bending and expansion	0.5	3.0
Flow stress	Yield Stress	1.5	0.5
	Ultimate Stress	1.5	0.5
Fracture toughness		2.0	0.33
Weld residual stress		0.1	1.5
Initiation time		3.0	0.5

Note that this sensitivity matrix includes initially distributed input parameters (flaw length, yield stress, ultimate stress, fracture toughness), and initially non-distributed parameters (flaw depth, load level, weld residual stress). The consideration of initially non-distributed parameters can be interpreted either that intentional variations of the latter parameters are proposed, or that these input parameters have an uncertainty that is not explicitly included in the probabilistic test case via the distribution functions. With this variation, the analysis goes beyond the scope of the uncertainty of initially distributed parameters, and one should treat the associated results separately from the other variations. The sensitivity analysis results are presented in Fig. 13 – the lines connecting initially distributed parameters are solid, the lines for initially non-distributed parameters are dashed.

5. Comparison and assessment of the sensitivity measure results

5.1. Classification and synopsis

All six approaches for the identification of sensitive parameters ended up in a conclusion of most relevant and less relevant parameters, with a certain ranking. For a better comparison (the parameters included in the study are not the same for all methods), we classify these outcomes into the group of high, medium, and low importance. The comparison of the sensitivity measure results for initially distributed parameters (basic variables), which correspond to the effect of parameter uncertainties on the estimate of failure probability, is summarized in Table 11.

The methods mostly agree on the ranking of high sensitivity (initiation time), medium sensitivity (initial flaw width), and low sensitivity (material parameters). According to the Direction Cosine method, the fracture toughness has a higher influence than the yield stress and the ultimate stress (and is therefore classified as 'Medium'), but a lower than the initial flaw length. The MPFP analysis is identifying the initial flaw length not as 'Medium', but as 'Low' parameter, but Fig. 11 allows us to argue that there is a clear curvature of the limit state towards this parameter.

The sample-based uncertainty also provides a sensitivity measure for initially non-distributed parameters, which is not reflecting uncertainties within the test case, but intentional variations. This approach identifies in addition to the initiation time the load stresses as most important. This observation indicates that the considered parameters of the individual methods differ: While the amplification ratio, the

Table 11
Parameter ranking comparison: Initiation time (t_I), initial flaw length (b_0), yield stress (σ_y), ultimate stress (σ_f), and fracture toughness (J_{Ic}).

Method	High	Medium	Low
Amplification Ratio	t_I	b_0	σ_y,σ_f, J_{Ic}
Direction Cosine	t_I	b_0, J_{Ic}	σ_y,σ_f
Degree of Separation	t_I	b_0	σ_y,σ_f, J_{Ic}
MPFP Analysis	t_I	–	σ_y,σ_f, J_{Ic}, b_0
Separation of Uncertainty	t_I	b_0	σ_y,σ_f, J_{Ic}
Sample-based uncertainty	t_I	b_0	σ_y,σ_f, J_{Ic}

direction cosine, the degree of separation, the MPFP analysis, and the degree of separation consider all basic variables and no additional input quantity; the sample-based method requires a choice of considered parameters, which may include initially distributed (basic variables the PFM problem) and initially non-distributed parameters.

Another remarkable point to make is the demand for additional input. Again, the first five approaches are entirely defined with the given distribution functions of the basic variables. The amplification ratio, the MPFP analysis, and the separation of uncertainty have a determined theoretical numerical value by the case definition, while the direction cosine and the degree of separation are additionally influenced by the sampling scheme of the simulation. The sample-based approach requires a manual selection and grouping of parameters and, in addition, the individual factors of the High and Low levels. This additional manual input of the method gives the opportunity to add supplementary information about the uncertainty of input parameters. However, it requires additional knowledge and effort, and the outcome is finally dependent on the included or excluded set of parameters.

5.2. Sensitivity perspective beyond the demonstration case

One should mention that the selected simplified application case ignores certain aspects of the reliability assessment of piping components in nuclear power plants. This subsection indicates which input parameters of PFM cases in nuclear applications are also relevant but were intentionally skipped from the demonstration case to reduce the complexity. Technically, what is discussed here resembles a sample-based sensitivity study as described in Section 4.6, since a modified version of the original demonstration case is studied and the effect on the estimate of failure probability is discussed.

The weld residual stress profile was assumed as an initially non-distributed quantity in the test case description, although weld residual profiles are a result of the manufacturing process and show statistical scattering in the field. Thus, the profile would be a possible candidate for initially distributed input parameters to consider the uncertainties. However, the validation of best-estimate weld residual stress profiles is a competitive strategy for the consideration of the related uncertainties. A more detailed consideration of weld residual stresses should also acknowledge the influence on the crack initiation rate since tensile stresses at the surface are relevant for this damage mechanism.

Beyond the influence of the uncertain weld residual stress profile, the crack growth rate itself is also affected by uncertainties, especially for stress corrosion cracking. Corrosive crack growth depends on material and medium, and large statistical scattering is observed in experiments, and the specification of crack growth relations with realistic uncertainties is challenging. Many approaches treat the crack growth rate parameters as fixed, which can also reflect a requirement in compliance with a code, or a conservative choice. However, this treatment hides intrinsic uncertainties of stress corrosion cracking, and it is worth questioning also assumptions of "initial" (initiated) cracks and their size, as well as the dependency of the crack growth rate with the stress intensity factor.

One important influence factor and mitigation measure for piping in nuclear power plants is the role of surveyance and inspection. The consideration of in-service inspections in probabilistic fracture mechanical simulations is a standard technique by assuming recurrent inspections with a specified time interval. The finding of indications in non-destructive testing is modeled by a probability of detection (POD) dependent on the flaw depth. Both inspection interval and POD curve offer the opportunity to study the influence of the parameters on the rupture probability and allow to measure the effectiveness of an inspection program.

$$POD(a) = \frac{\exp(\beta_0 + \beta_1 \ln a)}{1 + \exp(\beta_0 + \beta_1 \ln a)} \tag{15}$$

The parameters of this formulation are $\beta_0 = 0.8256$ and $\beta_1 = 0.8711$, respectively. The evaluation of the effect with inspection intervals 1 year, 5 years, and 10 years is shown in Fig. 14 (using the PROST result).

This comparison shows that a shorter inspection interval can reduce the rupture probability, and the result can support the decision-making for the maintenance program. A clear advantage of ISI which ensures lower leak and rupture probability values is demonstrated; it was received a reduction of about one order of magnitude in leak probability values with inspections of 5-year intervals.

An additional effect arises from the leak monitoring system, which potentially allows to identify small local leaks early and to repair the damaged parts before a rupture with severer consequences can occur. This leak-before-break concept is one important safety strategy in nuclear power plants, but the qualification is more relevant for middle and large diameter piping. The modelling of leak flow rates requires additional parameters with associated uncertainties (characterizing the crack morphology and the detection capability), and the applicability of leak-before-break in the presence of stress corrosion cracking is not accepted by all regulations, so this aspect was skipped in the test case definition.

The selected test is a small diameter, rather thin pipe in a PWR nuclear power plant subjected to stress corrosion cracking. The identified parameters of high influence might be typical for this type of piping, but one should mention that the chosen case triggers the identification of crack initiation time and flaw sizing. A main influencing factor for stress corrosive cracking degradation in middle and thick pipes, which have in general very low rupture probabilities; is the weld residual stress assumption.

6. Summary, conclusion, and outlook

In this paper, six different approaches for the ranking of influence parameters in probabilistic fracture mechanical simulations are presented, applied, and compared: The amplification ratio, the direction cosine, the degree of separation, the most probable failure point, the separation of uncertainty method, and the sample-based uncertainty method. These methods can be classified according to different attributes.

The amplification ratio, the separation of uncertainty, and the sample-based uncertainty approach rely on a scheme High/Base/Low parameter sets, which are varied one by one and a target quantity is evaluated. While the amplification ratio and sample-based uncertainty methods define the High/Low-levels based on the input parameter, the separation of uncertainty uses the computed target parameter.

The direction cosine method, the degree of separation, and the MPFP analysis lead to statements concerning the geometry of the basic variable space and the failure region. All these three methods, therefore, discuss the geometry in the space of standard normal variables (u-space). The coordinates of the vector between median or mean and

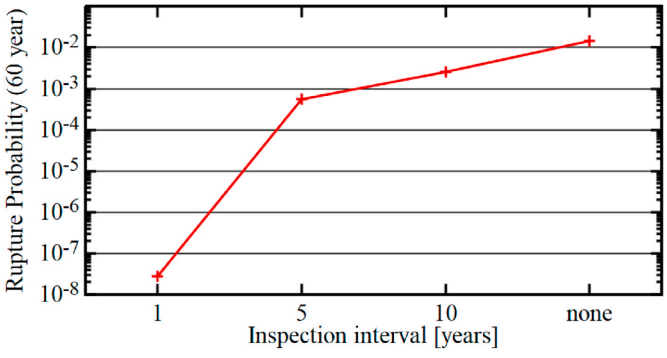

Fig. 14. Influence of the inspection interval on the estimate of rupture probability after 60 years.

the closest point in the failure region provide the information for the influencing parameters.

The proposed methods also differ in the required efforts for the evaluation. The direction cosine and the degree of separation can compute their ranking with the evaluations obtained in a Monte Carlo simulation. The MPFP analysis requires the computation of this specific point, which is part of certain computation schemes anyway. The amplification ratio and the separation of uncertainty require additional simulations similar to the original one (two times the number of basic variables for the amplification ratio, and about 500 times as much for the separation of uncertainty). The sample-based method requires also additional evaluations (two times the number of chosen groups), but also manual input in the form of individual parameter variations.

The evaluation showed also that certain methods have limitations concerning parameters of very high influence: The parameters are identified, but parameters that both have a very high influence cannot be compared adequately. The amplification ratio and the separation of uncertainty approach show this behavior; the parameter of the highest influence can be identified, but the influence cannot be quantified. This behavior is caused by the selected test case (mainly the damage mechanism stress corrosion cracking) but a single dominant influence parameter can also be present in other PFM applications.

The focus of this evaluation is the mathematical perspective of parameters and uncertainties influencing the estimate of pipe failure probability in a PFM analysis. Besides this approach, it is also relevant to consider the role of a sensitivity study during the design and operation of piping components, which can be done to find (efficient) ways to reduce risks associated with structural failures. In this case, not all sensitive (potentially risk-reducing) parameters can be controlled but are fixed constrained. In such an analysis, the role of damage mechanisms uncertainties as presented in the demonstration case is of minor importance, while the inspection strategy is a key interception point. However, also this risk-oriented approach would take profit if relevant uncertainties of not-controllable influence parameter are reduced.

The results and the survey of methods are a result of the IAEA CRP on pipe failure rates in AWCR, which has aimed to develop best practice guidelines for the assessment of reliability parameters. In this light, the analysis of the most influential parameters should be recommended for PFM analyses, since the information can be (dependent on the application case) equally important as the estimate of computed failure probability. The analysis of the sensitivity of input parameters is also of practical relevance in the modelling phase of a structure since the identified parameters can be compared with practical experience and failure events and reveal possibilities for parameter calibrations. This ability supports the PFM-based computation of failure rates for piping in advanced plants of Generation III/III+. The present comparative survey is a technical basis for the IAEA member states' application of sensitivity studies in PFM applications.

Declaration of competing interest

The authors declare that they have no known competing financial interests or personal relationships that could have appeared to influence the work reported in this paper.

Acknowledgement

Part of this work was conducted by the International Atomic Energy Agency (IAEA) in the frame of the Coordinated Research Project I31030 on "Methodology for Assessing Pipe Failure Rates in Advanced Water-Cooled Reactors (AWCRs)". Parts are funded by the German Federal Ministry of Economics and Energy (BMWi, Research grant RS1551). The supports are gratefully acknowledged. The authors thank the anonymous reviewers for their valuable comments.

References

[1] W.-C. Cheng, T. Sakurahara, S. Zhang, P. Farshadmanesh, S. Reihani, E. Kee, Z. Mohaghegh, K. Heckmann, J. Sievers, B. Lydell, C. Zammali, X.-X. Yuan, X. Duan, R. Alzbutas, G.-G. Lee, J.A. Karim, V. Morozov, C. Takasugi, T. Jevremovic, Review and categorization of existing studies on the estimation of probabilistic failure metrics for reactor coolant pressure boundary piping and steam generator tubes in, Nuclear Power Plants 118 (2020) 103105, https://doi.org/10.1016/j.pnucene.2019.103105. ISSN 0149-1970, Progress in Nuclear Energy.

[2] R. Rackwitz, Reliability analysis—a review and some perspectives, Struct. Saf. 23 (4) (2001) 365–395, https://doi.org/10.1016/S0167-4730(02)00009-7. ISSN 0167-4730.

[3] M. Kloos, und Berner, N.: SUSA Documentation. GRS-P-5 1–3 (2019). Version 4.2, Technical Report, Garching, Germany.

[4] D. Shim, C. und Harrington, D. Somasundaram, Sensitivity analysis methodology for probabilistic fracture mechanics output. Division II, structural mechanics in reactor technology (SMiRT-25), 2019. Charlotte, NC, USA, 2019 4-9 Aug.

[5] T. Sakurahara, S. Reihani, E. Kee, Z. und Mohaghegh, Global importance measure methodology for integrated probabilistic risk assessment, Proc. Inst. Mech. Eng. O J. Risk Reliab. 234 (2) (2020) 377–396, https://doi.org/10.1177/1748006X19879316.

[6] Eberhard Roos, Herter, Michael Karl-Heinz und Ringel, Evaluation of full scale pipe tests based on a probabilistic procedure, in: 18th International Conference on Structural Mechanics in Reactor Technology (SMiRT 18), 2005, 7-12 Aug 2005, Beijing, China.

[7] Klaus Heckmann, Jürgen Sievers, Arndt, Jens und Bläsius, Christoph: extension and application of the PROST Computer Code for deterministic and probabilistic leak-before-break assessment of pipes in vessels, GRS-422 (2016). ISBN 978-3-946607, Technical Report, Cologne, Germany.

[8] R.E. Melchers, A.T. Beck, Structural Reliability Analysis and Prediction, third ed., Wiley, Hoboken, NJ, 2018.

[9] A.E. Hami, B. Radi, Uncertainty and Optimization in Structural Mechanics, John Wiley & Sons, Hoboken, NJ, 2013.

[10] A.H.-S. Ang, W.H. Tang, Probability Concepts in Engineering Planning and Design, Volume II: Decision, Risk and Reliability, Chichester: Wiley, NY, 1984.

[11] Wang, M., Duan, X. and Kozulk, M.J., Benchmarking PRAISE-CANDU 1.0 with XLPR 1.0, Proceedings of the ASME 2013 Pressure Vessels & Piping Division Conference, PVP2013-98010, July 14-18, 2013, Paris, France.

[12] X. Duan, M. Wang, J. Kozulk, Acceptance criterion for probabilistic structural integrity assessment: prediction of the failure pressure of steam generator tubing with fretting flaw, Nucl. Eng. Des. 281 (2015) 154–162.

[13] G.E. Apostolakis, C. Guedes Soares, S. Kondo, Special Issue on Treatment of Aleatory and Epistemic Uncertainty, vol. 54, Reliability Engineering & System Safety, 1996 November/December, 2-3.

[14] T. Schimpfke, Fatigue Benchmark Study. NURBIM Final Report, WP-4 Appendix B, EURATOM Contract No. FIKS-CT-2001-00172, 2004.

[15] BOMEL Limited: probabilistic methods: uses and abuses in structural integrity, Contract Research Report 398 (2001), 0 7176 2238 X, Technical Report, United Kingdom, 2001. Item availability may be restricted.

[16] K. Heckmann, K. Ma, J. und Sievers, Probabilistic aspects on break preclusion assessment in nuclear piping, 2015, 41st MPA-Seminar, 5-6 October 2015, Stuttgart, Germany.

[17] Xinjian Duan, Klaus Heckmann, Robertas Alzbutas, Ahn und, Dong-hyun: phase 1 PFM benchmark of the IAEA CRP I31030 pipe failure rate estimate, in: 3rd International Seminar on Probabilistic Methodologies for Nuclear Applications, 22-24 Oct 2019, 2019. Rockville, MD, USA.

[18] K. Heckmann, J. Sievers, Integrity assessment of piping with the PROST code, in: Paper Presented at Enlarged Halden Program Group Meeting, Lillehammer, September 2017. Norway.

[19] K. Heckmann, J. Sievers, Code development for piping integrity assessment with respect to new German safety standard, in: Paper Presented at SMiRT-23, Paper 148, 2015. Manchester.

[20] M. Bergman, B. Brickstad, F. Nilsson, A Procedure for Estimation of Pipe Break Probabilities Due to IGSCC", SAQ/FoU-Report 97/06, SAQ Kontroll AB, Stockholm, Sweden, 1997.

[21] Alzbutas R., "Approaches of Risk Measures Minimization and Application to Inspection", 13th International Conference on Probabilistic Safety Assessment and Management (PSAM 13) 2-7 October, 2016. Sheraton Grande Walkerhill Seoul, Korea. p. 1-14.

[22] Dundulis G., Alzbutas R., "Pipe rupture and inspection sensitivity analysis", Proceedings of the 52th ESReDA Seminar, May 30-31, 2017, Kaunas, Lithuania. ISBN 978-92-79-73870-8. p. 108-116.

[23] X. Duan, M. Wang, M.J. Kozluk, Benchmarking PRAISE-CANDU 1.0 with nuclear risk based inspection methodology Project fatigue cases, J. Pressure Vessel Technol. 137 (April 2015).